SUPPLEMENTARY INFORMATION

Rett Syndrome Mutation MeCP2 T158A Disrupts Methyl-DNA Binding, Protein Stability and ERP Responses

Darren Goffin, Megan Allen, Le Zhang, Maria Amorim, I-Ting Judy Wang, Arith-Ruth S. Reyes, Amy Mercado-Berton, Caroline Ong, Sonia Cohen, Linda Hu, Julie A. Blendy, Gregory C. Carlson, Steve J. Siegel, Michael E. Greenberg and Zhaolan (Joe) Zhou

Figure S1

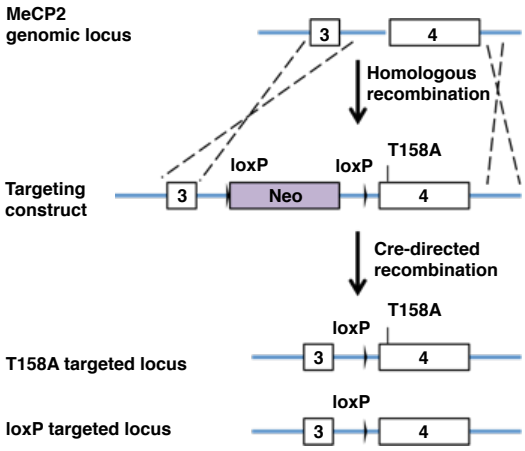

Supplementary Figure 1: Generation of MeCP2 T158A and loxP knockin mice

Targeting strategy to generate MeCP2 T158A and loxP knockin mice. The genomic region surrounding *Mecp2* exons III and IV was targeted for homologous recombination using a construct in which the floxed neomycin positive selection cassette (Neo) was inserted in a non-conserved region of intron III. The location of the mutation in exon IV to create T158A is indicated. Since we were testing for the effects of a single nucleotide mutation, two lines of mice were generated: those with and those without the T158A mutation. Both lines contained floxed loxP sites. Following production of chimera, the Neo cassette was removed using *EIIa-cre* mice. The targeted alleles after cre-mediated removal of the Neo cassette are illustrated.

Figure S2

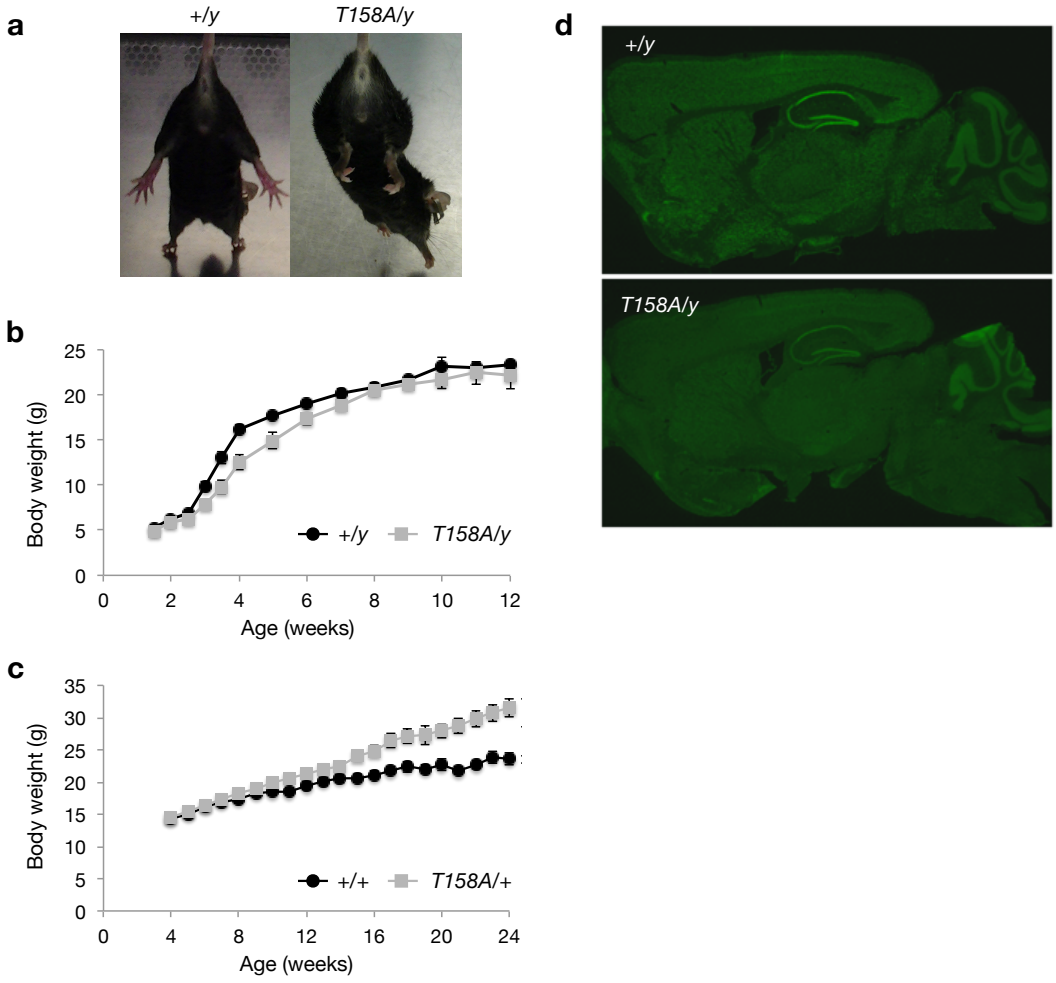

Supplementary Figure 2: Characterization of MeCP2 T158A mice

a. Stereotypical hindlimb clasping upon tail suspension in an *Mecp2*$^{T158A/y}$ mouse at 13 weeks of age versus an age-matched *Mecp2*$^{+/y}$ littermate. **b.** Body weights in male *Mecp2*$^{T158A/y}$ mice (n = 11; $F_{1,252}$ = 27.75, p<0.0001, two-way ANOVA) compared to WT littermates (n = 9). Points represent mean ± SEM. **c.** Body weights in female *Mecp2*$^{T158A/+}$ mice (n = 7; $F_{1,242}$ = 176.77, p<0.0001, two-way ANOVA) compared to *Mecp2*$^{+/+}$ littermates (n = 7). Points represent mean ± SEM. **d.** Normal gross brain anatomy in *Mecp2*$^{T158A/y}$ mice compared to *Mecp2*$^{+/y}$ mice. Sagittal sections were stained with an antibody against MeCP2.

Figure S3

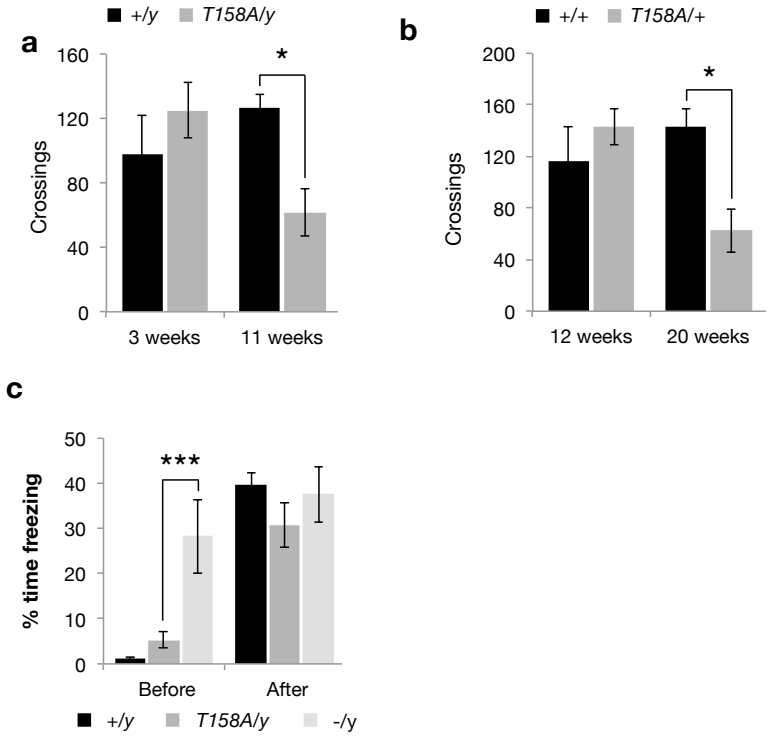

Supplementary Figure 3: Behavioral phenotypes of *Mecp2*$^{T158A/y}$ mice

a. Locomotor activity measured in male mice using an open field assay at 11 and 3 weeks of age. Bars represent mean ± SEM (n = 6 for *Mecp2*$^{+/y}$ and n = 8 for *Mecp2*$^{T158A/y}$). * *p*-value < 0.05; two-tailed t-test with Bonferroni correction. **b.** Locomotor activity measured in female mice using an open field assay at 20 and 12 weeks of age. Bars represent mean ± SEM (n = 5 for *Mecp2*$^{+/+}$ and n = 5 for *Mecp2*$^{T158A/+}$). * *p*-value < 0.05; two-tailed t-test with Bonferroni correction. **c.** Percentage time spent freezing in *Mecp2*$^{+/y}$ (n = 33), *Mecp2*$^{T158A/y}$ (n = 16) and *Mecp2*$^{-/y}$ mice (n = 12) prior to, and subsequent to tone and shock on training day of fear conditioning procedure. *Mecp2*$^{-/y}$ mice freeze significantly more than WT or *Mecp2*$^{T158A/y}$ mice prior to experimentation obviating them from further analysis. Bars represent mean ± SEM. *** *p*-value < 0.001; two-tailed t-test with Bonferroni correction.

Figure S4.

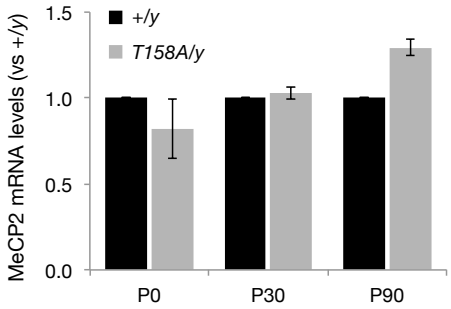

Supplementary Figure 4: MeCP2 mRNA expression is not affected by T158A mutation

MeCP2 mRNA levels in *Mecp2*$^{T158A/y}$ mice (n = 3) at P0, P30 or P90 compared to *Mecp2*$^{+/y}$ littermates (n = 3). Bars represent mean ± SEM. Statistics performed using one-sample t-tests.

Figure S5

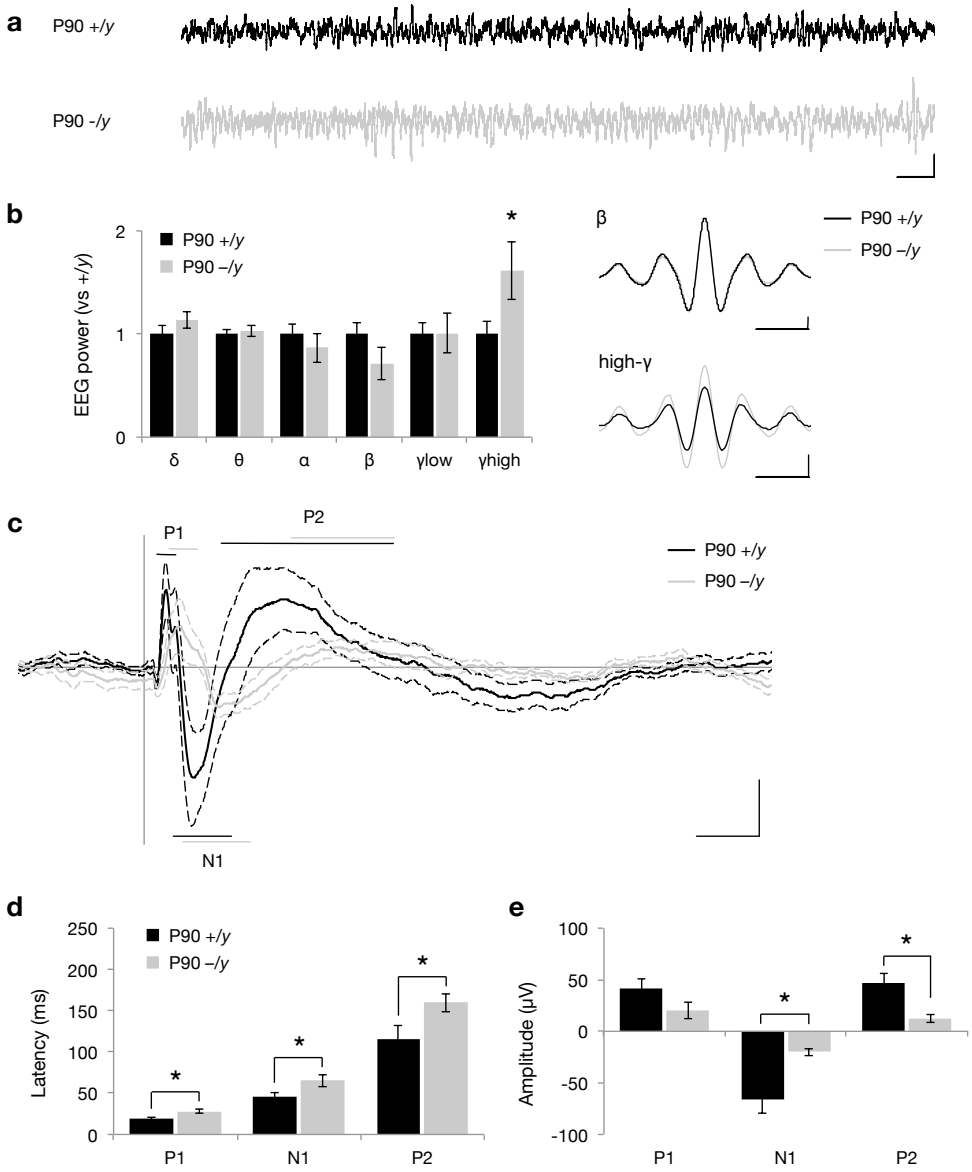

Supplementary Figure 5: *Mecp2*-null mice exhibit alterations in auditory-evoked ERPs

a. Representative EEG traces of awake, freely mobile mice. Scale bar corresponds to 1 second (horizontal) and 200 μA (vertical). **b.** Basal EEG power measurements in *Mecp2*$^{-/y}$ mice (n = 8) and *Mecp2*$^{+/y}$ littermates (n = 8). Bars represent mean ± SEM. * *p*-value < 0.05; two-tailed t-test with Bonferroni correction. Insets show β and high-γ mean amplitudes across EEG recordings. Scale bars represent one oscillation cycle (horizontal) and 20 μA (vertical). **c.** Grand average ERPs following 85-dB sound presentation. Traces represent mean amplitude (solid line) ± SEM (dashed lines). The characteristic polarity peaks P1, N1 and P2 are highlighted with straight lines with the length indicating latency range. Scale bar corresponds to 50 ms (horizontal) and 20 μA (on vertical). **d.** Latencies and **e.** amplitudes of ERP peaks. Bars represent mean ± SEM. * *p*-value < 0.05; two-tailed t-test with Bonferroni correction.

Figure S6

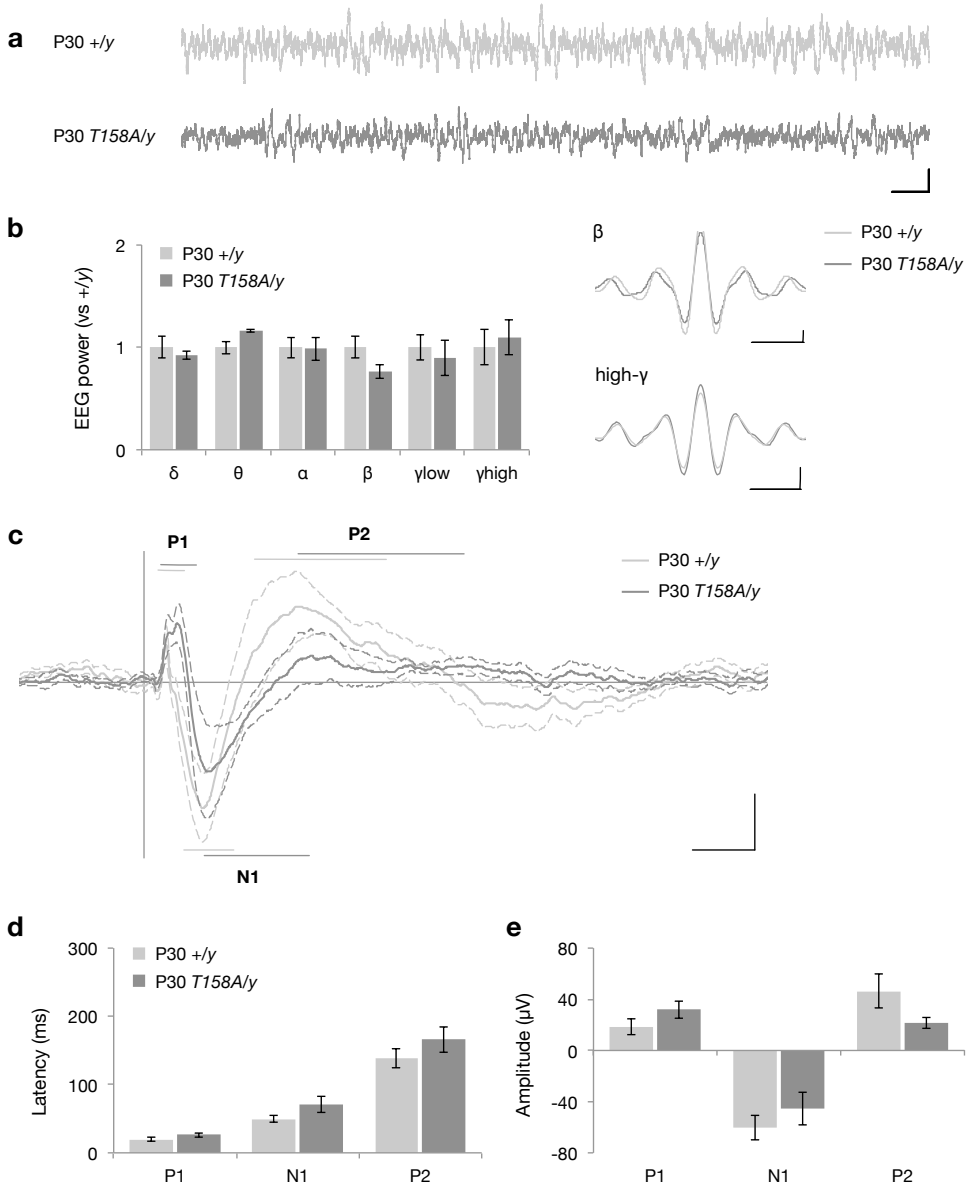

Supplementary Figure 6: Auditory-evoked ERPs are not affected in *Mecp2*$^{T158A/y}$ mice at P30

a. Representative EEG traces of awake, freely mobile mice. Scale bar corresponds to 1 second (horizontal) and 200 μA (vertical). **b.** Basal EEG power measurements in P30 *Mecp2*$^{T158A/y}$ mice (n = 7) and *Mecp2*$^{+/y}$ littermates (n = 8). Bars represent mean ± SEM. * p-value < 0.05; two-tailed t-test with Bonferroni correction. Insets show β and high-γ mean amplitudes across EEG recordings. Scale bars represent one oscillation cycle (horizontal) and 20 μA (vertical). **c.** Grand average ERPs following 85-dB sound presentation. Traces represent mean amplitude (solid line) ± SEM (dashed lines). The characteristic polarity peaks P1, N1 and P2 are highlighted with straight lines with the length indicating latency range. Scale bar corresponds to 50 ms (horizontal) and 20 μA (on vertical). **d.** Latencies and **e.** amplitudes of ERP peaks. Bars represent mean ± SEM. Statistics performed using two-tailed t-tests with Bonferroni correction.

Figure S7

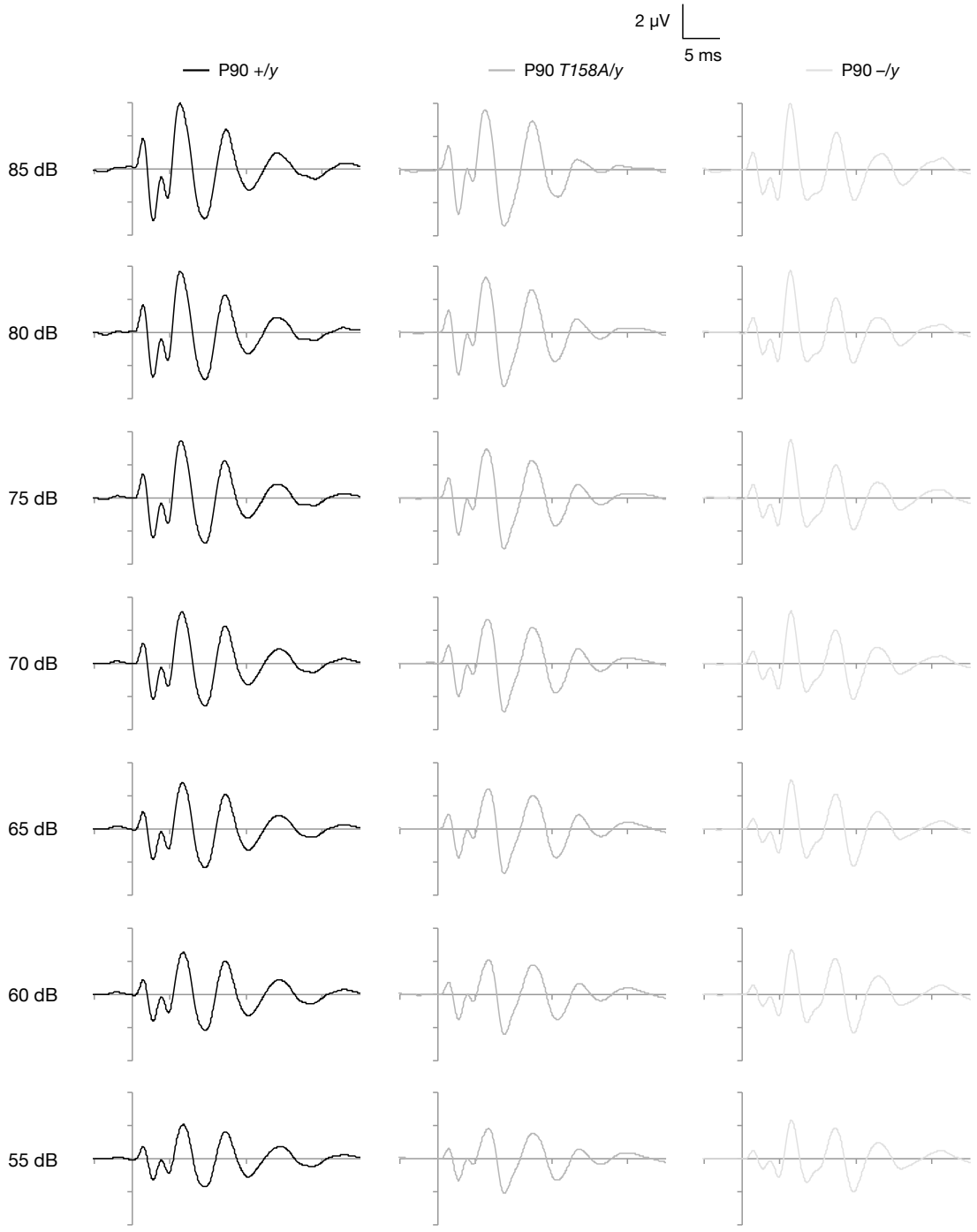

Supplementary Figure 7: Auditory brainstem responses

Auditory brain stem responses from P90 *Mecp2*$^{+/y}$, *Mecp2*$^{T158A/y}$ and *Mecp2*$^{-/y}$ mice. Mice were presented with 4,000 white-noise clicks (3 ms duration, 125 ms inter-stimulus interval) ranging from 85-dB to 55 dB sound pressures. ABR responses decreased to a similar extent in all three genotypes with decreasing sound pressure.

Figure S8

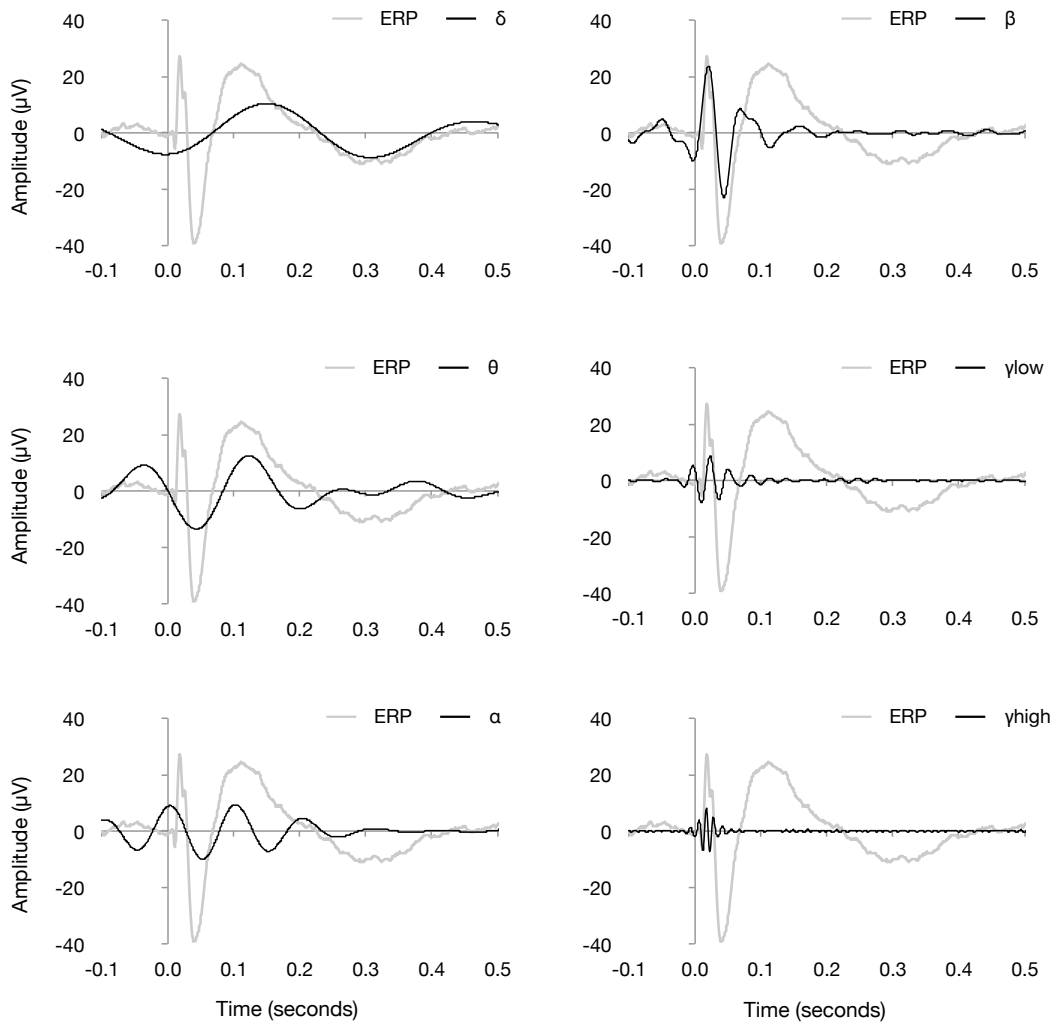

Supplementary Figure 8: Oscillation changes occur for multiple cycles during ERPs

EEG traces were band pass filtered in frequency ranges defined as δ (2-4 Hz), θ (4-8 Hz), α (8-12 Hz), β (12-30 Hz), γlow (30-50 Hz) and γhigh (70-140 Hz). The P1 peak consists primarily of oscillations in the β, low- and high-γ ranges. The N1 peak is composed primarily of α and β frequencies. The P2 peak is primarily composed of δ and θ frequencies.

Figure S9

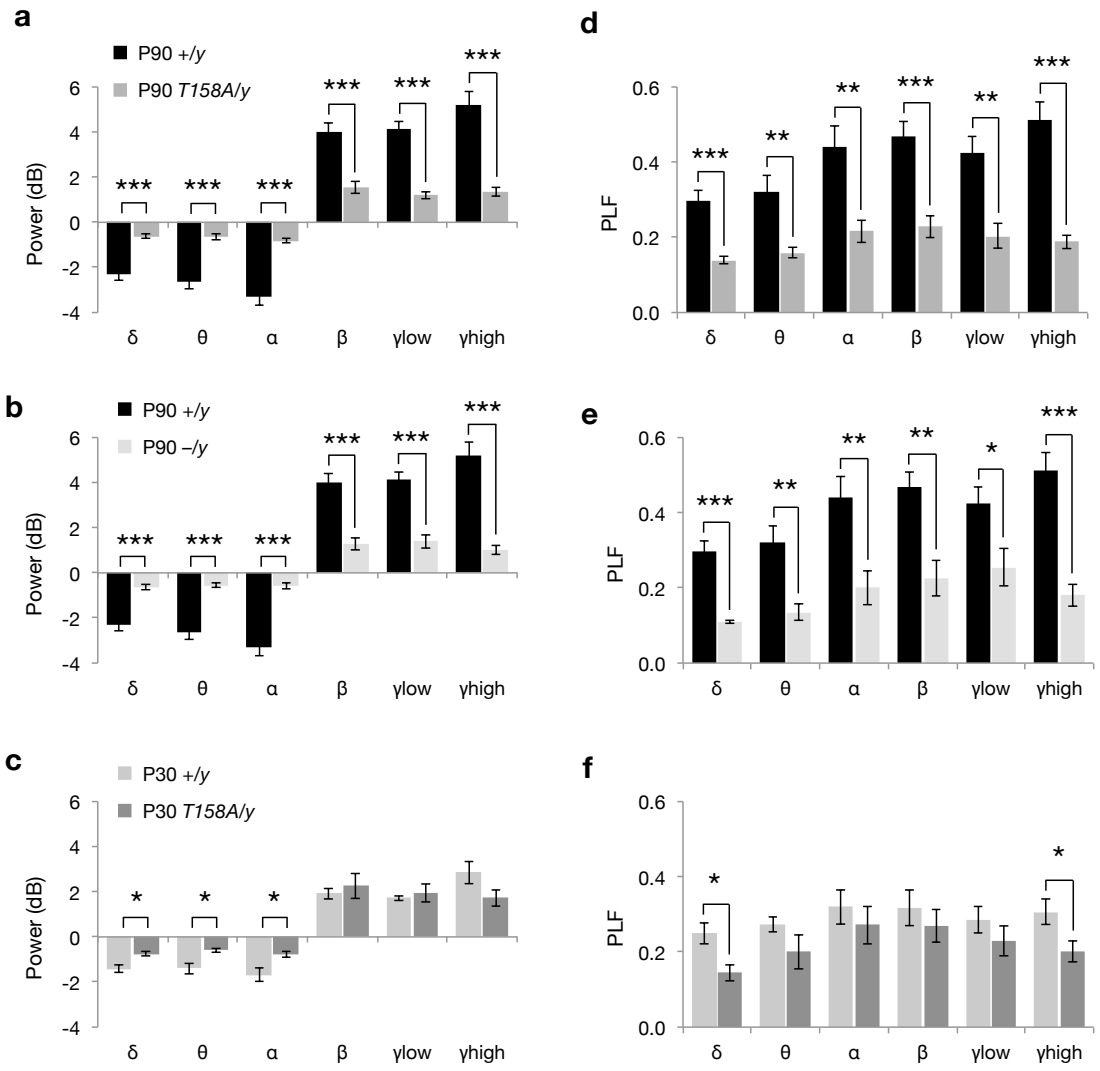

Supplementary Figure 9: Quantification of event-related power and PLF changes

a. Event-related power changes in *Mecp2*$^{T158A/y}$ mice and *Mecp2*$^{+/y}$ littermates at P90. **b.** Event-related power changes in *Mecp2*$^{-/y}$ mice and *Mecp2*$^{+/y}$ littermates at P90. **c.** Event-related power changes in *Mecp2*$^{T158A/y}$ mice and *Mecp2*$^{+/y}$ littermates at P30. **d.** Event-related PLF in *Mecp2*$^{T158A/y}$ mice and *Mecp2*$^{+/y}$ littermates at P90. **e.** Event-related PLF in *Mecp2*$^{-/y}$ mice and *Mecp2*$^{+/y}$ littermates at P90. **f.** Event-related PLF in *Mecp2*$^{T158A/y}$ mice and *Mecp2*$^{+/y}$ littermates at P30. Bars represent mean ± SEM. * p-value < 0.05, ** < 0.01 and *** < 0.001; two-tailed t-test with Bonferroni correction.

Figure S10

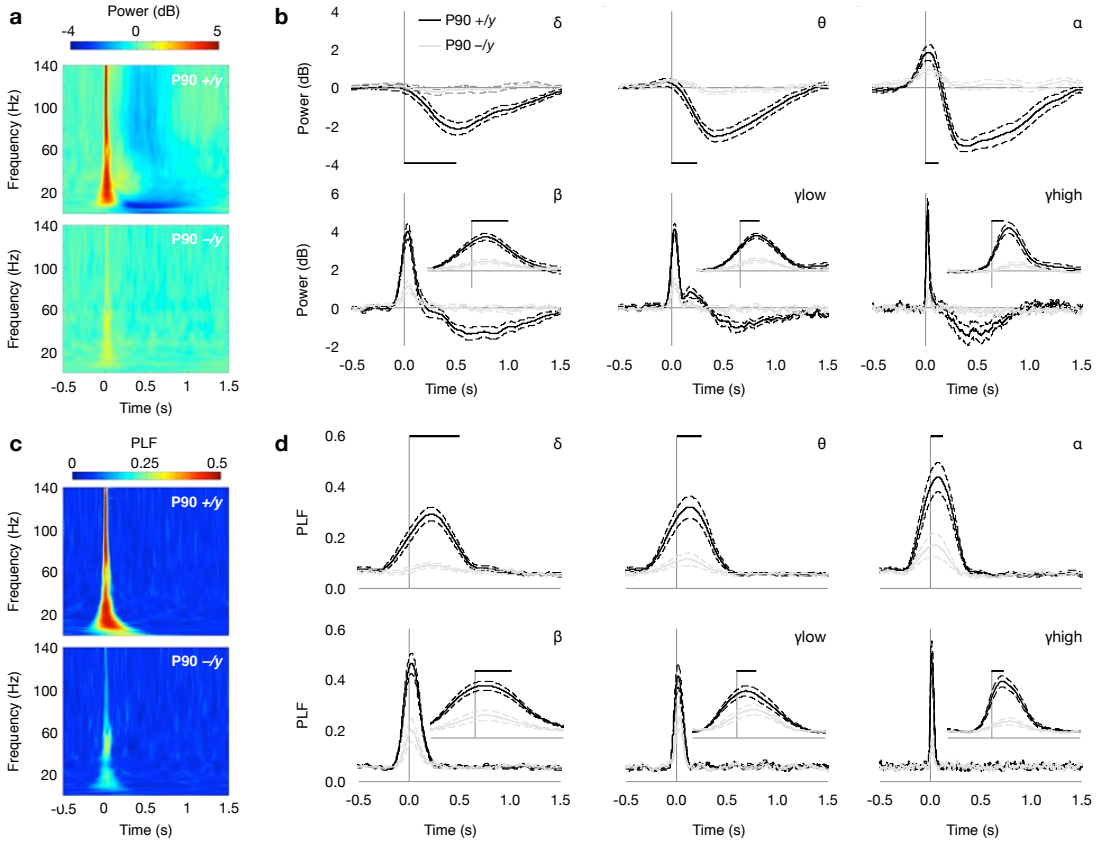

Supplementary Figure 10: Time-frequency analysis in *Mecp2*$^{-/y}$ mice

a. Time-frequency plots showing event-related power in response to 85-dB white-noise clicks. Time is plotted on the abscissa (where $t = 0$ at sound presentation) and frequency on the ordinate. Color represents mean power with warmer colors corresponding to an increased power and cooler colors representing decreased power compared to pre-stimulus baseline. **b.** Event-related power changes were separated into δ-, θ-, α-, β-, low γ- and high γ-frequency bands. Scale bars represent one oscillation cycle for the lowest frequency (longest duration cycle) in each band. Insets show traces on expanded time scale. Data are presented as mean power ± SEM. **c.** Time-frequency plots showing changes in phase locking factor (PLF) as a function of time and frequency. Color represents PLF with warmer colors corresponding to a higher PLF or lower circular variance in EEG phase across trials. **d.** PLF was separated into frequency bands. Data are presented as mean PLF ± SEM.

Figure S11

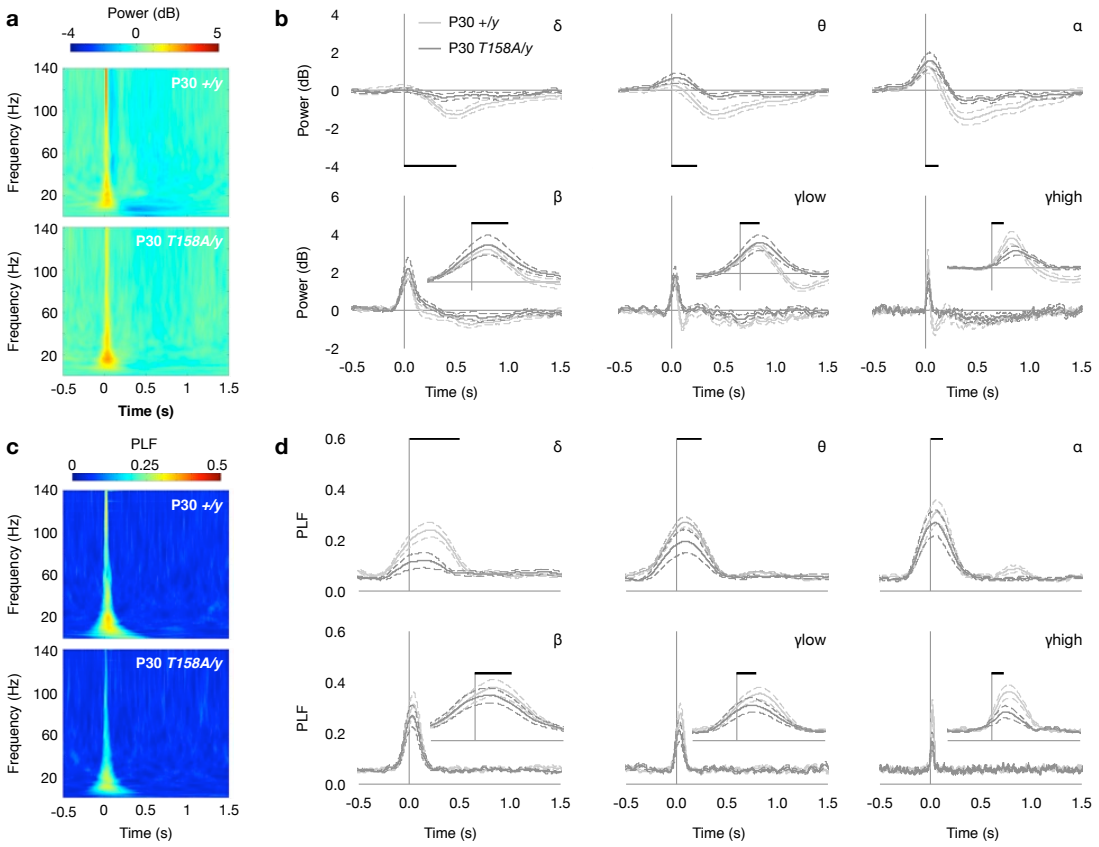

Supplementary Figure 11: Time-frequency analysis in P30 *Mecp2*$^{T158A/y}$ mice

a. Time-frequency plots showing event-related power in response to an 85-dB white noise clicks. Time is plotted on the abscissa (where $t = 0$ at sound presentation) and frequency on the ordinate. Color represents mean power with warmer colors corresponding to an increased power and cooler colors representing decreased power compared to pre-stimulus baseline. **b.** Event-related power changes were separated into δ-, θ-, α-, β-, low γ- and high γ-frequency bands. Scale bars represent one oscillation cycle for the lowest frequency (longest duration cycle) in each band. Insets show traces on expanded time scale. Data are presented as mean power ± SEM. **c.** Changes in phase locking factor (PLF) as a function on time and frequency. Color represents PLF with warmer colors corresponding to a higher PLF or lower circular variance in EEG phase across trials. **d.** PLF was separated into frequency bands. Data are presented as mean PLF ± SEM.

Figure S12

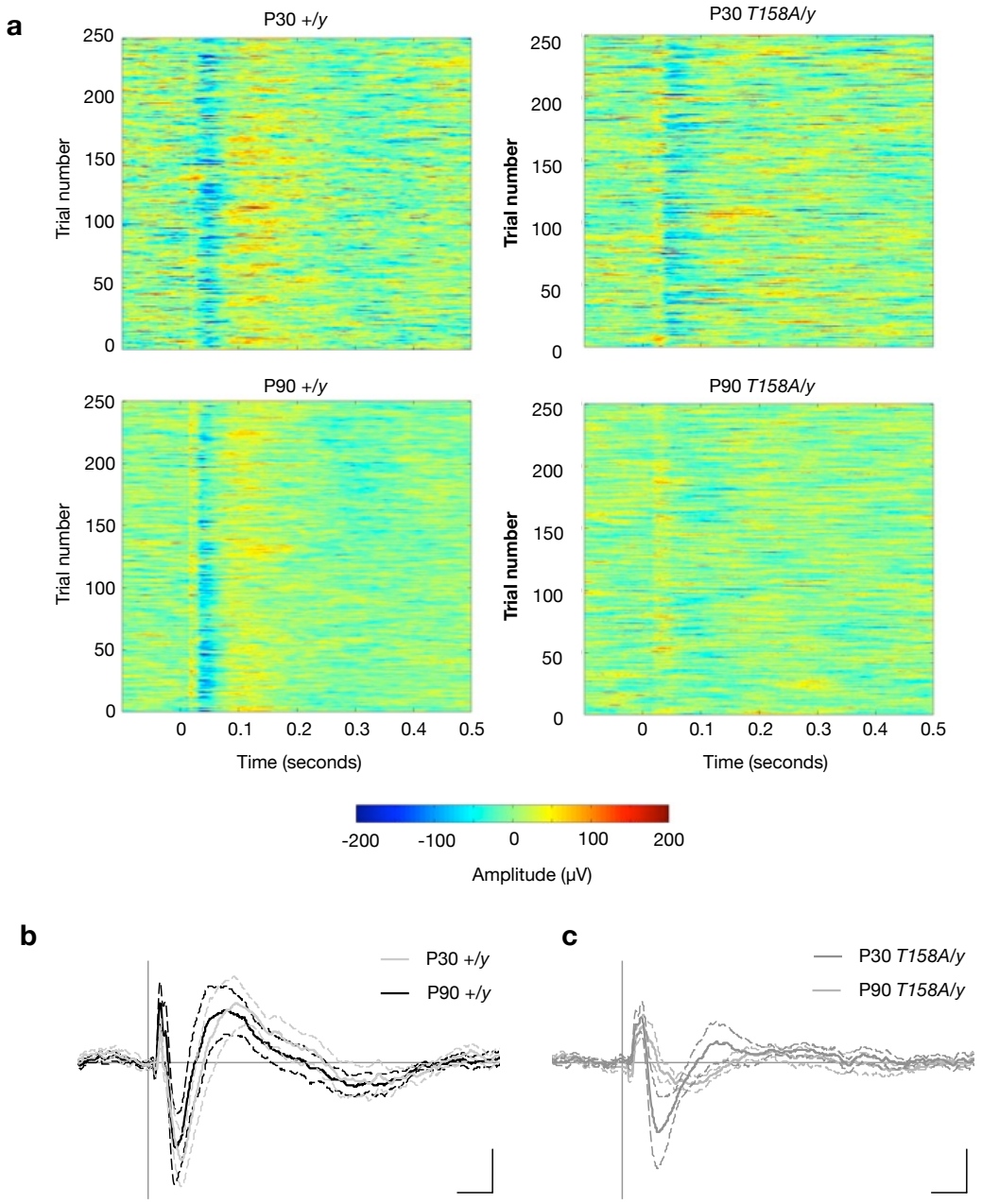

Supplementary Figure 12: Auditory-evoked ERPs in *Mecp2*$^{+/y}$ and *Mecp2*$^{T158A/y}$ mice

a. Heat maps showing ERPs recorded following presentation of 250 white-noise clicks (10 ms duration, 85-dB sound pressure, 4 second interstimulus intervals). Time is shown on the abscissa and trial number on the ordinate with the color representing EEG amplitude (μV). **b.** Grand average ERPs for *Mecp2*$^{+/y}$ mice at P30 and P90. Traces represent mean amplitude ± SEM. Scale bar corresponds to 50 ms (horizontal) and 20 μA (on vertical). **c.** Grand average ERPs for *Mecp2*$^{T158A/y}$ mice at P30 and P90. Traces represent mean amplitude ± SEM. Scale bar corresponds to 50 ms (horizontal) and 20 μA (on vertical).

Figure S13

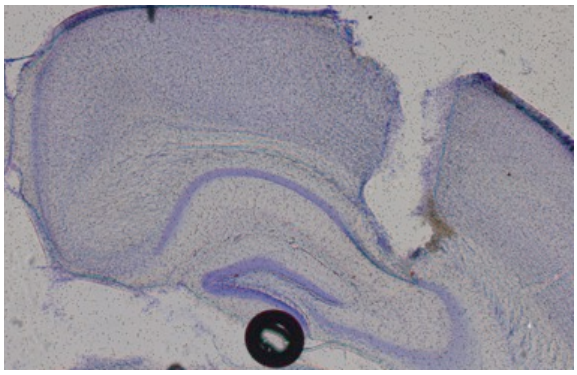

Supplementary Figure 13: EEG electrode placement in hippocampus

Representative 100 μm brain section with Nissl staining showing electrode placement in hippocampus.

Figure S14

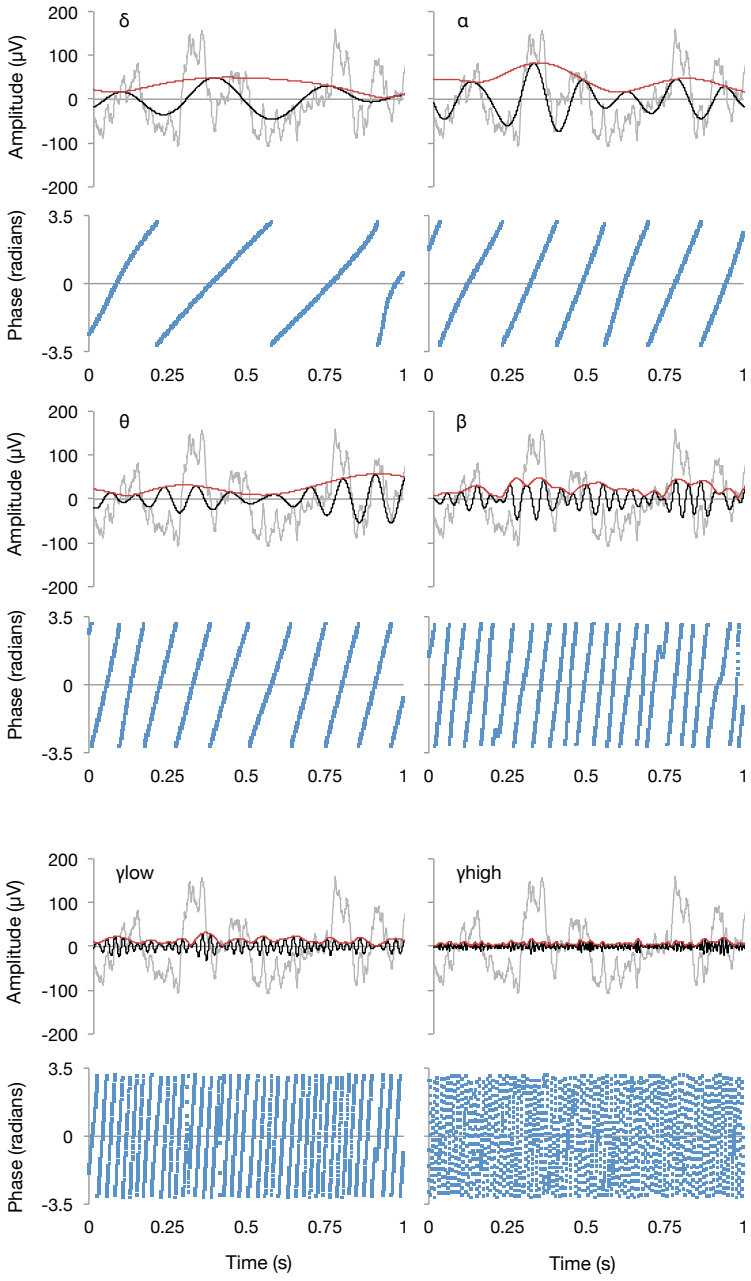

Supplementary Figure 14: EEG analysis using Hilbert transform

Time-frequency analysis was calculated using Hilbert transform to generate instantaneous amplitude and phase measurement. Traces show 1 second raw EEG trace in gray from P90 *Mecp2*$^{+/y}$ (WT) mice with the trace filtered at δ (2-4 Hz), θ (4-8 Hz), α (8-12 Hz), β (12-30 Hz), γlow (30-50 Hz) and γhigh (70-140 Hz) frequencies and shown in black. Amplitude envelope calculated from Hilbert transform is shown in red. Phase calculation is shown underneath with values expressed in radians.

Supplementary Video 1: Motor deficits in *Mecp2*$^{T158A/y}$ mice

Example video shows locomotor deficits in male *Mecp2*$^{+/y}$ (starts at bottom left), *Mecp2*$^{T158A/y}$ (starts at top right) and *Mecp2*$^{-/y}$ mice (starts at top left) at 11 weeks of age. Both *Mecp2*$^{T158A/y}$ and *Mecp2*$^{-/y}$ mice show decreased locomotor activity and aberrant gait with splaying of hind limbs upon movement.